OPEN ACCESS
JOURNAL OF ADVANCED DIELECTRICS
Vol. 11, Nos. 4 and 5 (2021) 2160014 (6 pages)
© The Author(s)
DOI: 10.1142/S2010135X21600146

XI'AN JIAOTONG UNIVERSITY
World Scientific
www.worldscientific.com

Optical properties of $Sr_xBa_{1-x}Nb_2O_6$ nanoscale films (x = 0.5 and 0.61) grown by RF-cathode sputtering in an oxygen atmosphere

S. V. Kara-Murza*, K. M. Zhidel†, N. V. Korchikova*, Yu. V. Tekhtelev*,
A. V. Pavlenko†,‡,§ and L. I. Kiseleva‡

*Lugansk State Pedagogical University
No. 2 Oboronnaya Street, Lugansk 91000, Ukraine

†Research Institute of Physics, Southern Federal University
No. 194 Stachki Avenue, Rostov-on-Don 344090, Russia

‡Federal State Budgetary Institution of Science "Federal Research Centre
The Southern Scientific Centre of the Russian Academy of Sciences"
No. 41 Chekhova Street, Rostov-on-Don 344090, Russia

§antvpr@mail.ru

Received 15 April 2021; Revised 8 June 2021; Accepted 15 June 2021; Published 17 August 2021

The research findings of the phase composition, nanostructure and optical properties of strontium–barium niobate thin films are discussed. $Sr_xBa_{1-x}Nb_2O_6$ nanosized films (x = 0.5 and 0.61) were characterized by XRD, SEM and AFM studies. Reflective multi-angle ellipsometry and spectrophotometry were used to determine the optical parameters (refractive index, its dispersion, and thickness of the damaged surface layer) of thin films. It was shown that SBN-50 and SBN-61 thin films were grown *c*-oriented on Al_2O_3 (0001) and heteroepitaxial on MgO (001) substrates. The increase of refractive index, approaching its maximum value in the bulk material for a given composition as the film thickness increases, is observed.

Keywords: Ellipsometry; optical parameters; strontium–barium niobates; thin films.

J. Adv. Dielect. Downloaded from www.worldscientific.com
by 95.24.11.130 on 10/16/21. Re-use and distribution is strictly not permitted, except for Open Access articles.

1. Introduction

In recent decades, the rapid development of telecommunication systems has contributed to the fact that in physical materials science, much attention has been paid to the development of production technology, synthesis and establishment of regularities in the formation of physical properties in active materials. Such materials have high values of dielectric controllability and electro-optical effect. At the same time, there are no toxic elements in their composition.[1]

Strontium–barium niobate, $Sr_xBa_{1-x}Nb_2O_6$ (SBN_x, x is the stoichiometric coefficient), solid solutions are among the most interesting in the aspects noted above.[2] The phase transition from the tetragonal ferroelectric (FE) phase (*P*4*bm*) to the paraelectric (PE) (*P*4*b*2) phase increases with decreasing Sr^{2+} content.[3] The phase transition is accompanied by anomalous behavior in dielectric and optical properties, lattice dynamics and structural characteristics. One can vary the properties of these materials over a wide range by doping or changing the composition. It has been studied experimentally and theoretically in sufficient detail in large SBN_x crystal samples. In the case of nanosized thin films, in the production of ones, wherein the deformation engineering effects make a large contribution,[3] these studies were carried out fragmentarily and are contradictory in some cases. This may be due to different conditions for obtaining objects. The probabilistic settlement of A_1 and A_2 channels in the tetragonal tungsten–bronze-type structure[1] with Sr^{2+} and Ba^{2+} cations is the objects' feature. According to most authors, this leads to the manifestation of relaxor properties in these materials and the peculiar specificity of their domain structure, described, for example, in Ref. 4.

To analyze the optical characteristics of thin films (refractive index, its dispersion, thickness of the damaged surface layer and/or film–substrate boundary layer, etc.) is to establish valuable information both from the viewpoint of practical application and from the theoretical positions. Ellipsometry can be[1–3] the most effective method for solving the assigned tasks, despite a number of technical difficulties arising in the interpretation of measurement results. Ellipsometry is one of the most sensitive optical methods to examine the surface of solids, based on the registration of changes in the parameters of the polarization ellipse of elliptically polarized light when it is reflected from the surface. The change in the parameters of the polarization ellipse occurs due to the interaction of electromagnetic radiation with the atoms of matter. This is characterized by ellipsometric angles ψ and Δ (φ is the

§Corresponding author.

This is an Open Access article published by World Scientific Publishing Company. It is distributed under the terms of the Creative Commons Attribution 4.0 (CC BY) License which permits use, distribution and reproduction in any medium, provided the original work is properly cited.

J. Adv. Dielect. Downloaded from www.worldscientific.com
by 95.24.11.130 on 10/16/21. Re-use and distribution is strictly not permitted, except for Open Access articles.

incidence angle): the ψ angle is associated with a change in the geometric characteristics of the polarization ellipse, and the Δ angle is associated with a change in the phases of the elliptically polarized light components when it is reflected from the surface.

The high sensitivity and information content of the ellipsometric method are due precisely to the fact that the change in the phases of the elliptically polarized wave components is recorded along with the change in the intensity during reflection. Ellipsometric measurements become especially important when studying the properties of thin and ultrafine heterostructures, which include single-layer coatings, taking into account the damaged surface layer and possible transition (buffer) layer in the "film–substrate" system of different nature and function. It should be noted that ellipsometry allows one to take into account the factor of possible anisotropy for the investigated surface.

In this paper, the research results of the phase composition, nanostructure and optical properties of strontium–barium niobate thin films with $Sr_{0.5}Ba_{0.5}Nb_2O_6$ (SBN-50) and $Sr_{0.61}Ba_{0.39}Nb_2O_6$ (SBN-61) compositions are presented. Thin films were grown *c*-oriented on Al_2O_3 (0001) (Ref. 4) substrates and heteroepitaxial on MgO (001) (Ref. 5) substrates.

2. Experimental Procedures

Solid solution of stoichiometric composition $Sr_{0.61}Ba_{0.39}Nb_2O_6$ was obtained at the Prokhorov Institute of General Physics, Russian Academy of Sciences, by solid-phase synthesis at a temperature of 1200 °C from the initial components $SrCO_3$, $BaCO_3$ and Nb_2O_5 of high-purity grade. Ceramic target of d = 50 mm and h = 3 mm was made in the Department of Intelligent Materials and Nanotechnology of the Research Institute of Physics, Southern Federal University (by sintering in an air atmosphere at T = 1350 °C for 2 h, the relative density of the resulting ceramics was ~92%). Ceramic target of stoichiometric composition $Sr_{0.5}Ba_{0.5}Nb_2O_6$ was produced in the Department of Intelligent Materials and Nanotechnology of the Research Institute of Physics, Southern Federal University in the same way.

Gas-discharge RF sputtering of SBN-50 and SBN-61 heteroepitaxial films was carried out at the Plasma 50 SE facility. MgO (001) single crystal 0.5-mm-thick (MT Corporation, USA) and Al_2O_3 (0001) 0.5-mm-thick (MT Corporation, USA) were used as the substrates. The substrate initial temperature was 400 °C, the pressure of pure oxygen in the chamber was 0.5 Torr, the RF power was 110 W on the MgO substrates during the film deposition. On the Al_2O_3 substrates, the RF power was 140 W. The target–substrate distance was 12–15 mm in all cases.

The film thickness was calculated from the deposition time (growth rate of ~5.5–6 nm/min). The film composition is preserved within the framework of the method used, and the film is not doped with structural elements.

The measurements were conducted on films, the deposition times of which were 30 min for SBN-50 on Al_2O_3 and 5, 10 and 115 min, respectively, for SBN-61 films on MgO.

Optical transmission spectra and ellipsometry were used to determine the thickness and profile of thin films, the refractive index and its dispersion. Ellipsometric measurements were performed using multi-angle reflective ellipsometer at helium–neon laser wavelength of λ = 632.8 nm. Ellipsometric angles ψ and Δ are calculated from the measured azimuths of the input arm polarizer of ellipsometer and the output arm analyzer. The azimuth measurement accuracy is 30′. Additional optical transmission spectra were recorded in the wavelength range of 200–1000 nm at room temperature using Shimadzu UV-2450 spectrophotometer.

3. Methods for Processing the Results of Ellipsometric and Spectrophotometric Measurements

We proposed the combined use of reflective multi-angle ellipsometry and spectrophotometry to determine the entire spectrum of optical characteristics of thin films. The developed appropriate methods to process the measurement results are presented in the literature.[2–3] Ellipsometric angles ψ and Δ, obtained from the measurements at fixed wavelength, are functions of the incidence angle ϕ of elliptically polarized light, its wavelength λ, optical parameters of the film and substrate, film thickness and possible additional layers. Determining film characteristics at known substrate parameters is reduced to solving the basic ellipsometry equation with regard to these parameters,

$$e^{i\Delta}\mathrm{tg}\psi = \frac{R^{(p)}}{R^{(s)}}, \tag{1}$$

where $R^{(p)}$ and $R^{(s)}$ are amplitude reflection coefficients of p- and s-polarized components of elliptically polarized incident electromagnetic wave. Expressions for the reflection coefficients in Eq. (1) are written using the corresponding scattering matrix. The matrix components are determined by model adequate to the test the film–substrate system.

The reflecting surface can be considered as a single-layer homogeneous and isotropic transparent film on transparent substrate in the zero approximation. The problem of determining the film parameters is solved by the method described in Refs. 2 and 3. The method is based on the features of dependences $\psi(\varphi)$ and $\Delta(\varphi)$: when the angle of incidence is equal to the main (principal) angle $\varphi = \varphi_0$, the ψ angle vanishes, and $\Delta = \pi/2$ or $3\pi/2$ [the main angle corresponds to the minimum of the $\psi(\varphi)$ observed dependence in real films]. Meanwhile,

$$\mathrm{Re}\left\{\frac{R^{(p)}(\varphi_0)}{R^{(s)}(\varphi_0)}\right\} = 0, \qquad \mathrm{Im}\left\{\frac{R^{(p)}(\varphi_0)}{R^{(s)}(\varphi_0)}\right\} = \pm 1. \tag{2}$$

The refractive index of the film is $n = n^{(0)} = \mathrm{tg}\ \varphi_0$ to the zero approximation of such model. Finding the film thickness

J. Adv. Dielect. Downloaded from www.worldscientific.com
by 95.24.11.130 on 10/16/21. Re-use and distribution is strictly not permitted, except for Open Access articles.

$d = d^{(0)}$ is reduced to solving the first part of Eq. (2) as square with regard to the value cos δ, where the argument is the phase incursion in the film:

$$\delta = \frac{4\pi}{\lambda} d\sqrt{n^2 - \sin^2\varphi_0} = \frac{4\pi}{\lambda} d_{\min}\sqrt{n^2 - \sin^2\varphi_0} + 2m\pi \quad (m = 0, 1, 2, \ldots). \tag{3}$$

If the film phase thickness nd is less than half the wavelength, then $m = 0$ and $d^{(0)} = d_{\min}$. Otherwise, it is necessary to find the order of interference m at the wavelength of 632.8 nm by independent methods — for example, by analyzing the interference extremes in the transmission spectrum. Further joint solution of Eq. (2) by successive approximations gives the values of the film parameters in the first approximation. The final correction of the results, which makes the calculated dependences $\psi(\varphi)$ and $\Delta(\varphi)$ as close as possible to the experimental ones, is carried out by introducing the surface disturbed and boundary film–substrate layers. This procedure is performed by optimization methods by sequentially introducing layers with one optimization parameter — the thickness and effective refractive index of the layer. The refractive index of the layer is given as some known function (most often linear). The boundary values of the function are determined by the refractive indices of the framing media.[2] Finally, knowing the film thickness, one can find the dispersion $n(\lambda)$ from the optical transmission spectrum (if the phase thickness of the transparent film nd is greater than $\lambda/4$, then the optical parameters can be estimated using only the characteristic transmission spectrum).

The anisotropy factor leads to additional changes in the interpretation of the ellipsometric results in anisotropic transparent films oriented in the direction parallel to the optical c-axis of uniaxial crystal. In this case, Eq. (1) retains its form,[1,4] but with a difference in the refractive indices for ordinary ray n_o and extraordinary one n_e, which is associated with change in the amplitude and phase of the reflected p-component of the electromagnetic wave. To a decisive extent, this deviation from the isotropic model is due to a change in the phase incursion in layer equal to

$$\delta^{(p)} = \frac{4\pi}{\lambda} d \frac{n_o}{n_e}\sqrt{n_e^2 - \sin^2\varphi_0^{(p)}}. \tag{4}$$

Assuming in the isotropic film model $n = n_o$ and comparing Eq. (4) with Eq. (3) at the given value of the main angle φ_0, one can estimate the error

$$\frac{\delta^{(p)}}{\delta} = \frac{n_o}{n_e}\frac{\sqrt{n_e^2 - \sin^2\varphi_0}}{\sqrt{n_o^2 - \sin^2\varphi_0}}. \tag{5}$$

arising from the analysis of ellipsometric data without taking into account the film anisotropy.

The refractive index is equal to n_o = 2.3–2.31 and n_e = 2.28–2.29 (Refs. 6 and 7) in strontium–barium niobate crystals for the considered compositions. Since in the zero approximation of the isotropic model φ_0 = arctg n_o = 66.5°, the ratio estimate for Eq. (5) gives a value of 0.999. Thus, the processing of the ellipsometric results for strontium–barium niobate films of the considered compositions, mainly oriented in the c-axis direction, can be performed using isotropic film model, taking $n = n_o$. For these reasons, the weak anisotropy of Al_2O_3 and MgO crystalline substrates oriented in the 001 direction can also be neglected.

4. Experimental Results and Discussion

It has been shown by ellipsometric measurements that all SBN films are characterized by growth direction, which is parallel to the optical c-axis direction of the crystal [incidence plane rotation of the probe beam does not change the ψ and Δ angle values (Ref. 1)). Figures 1 and 2 show the optical transmission spectra of SBN-50/Al_2O_3 and SBN-61/MgO thin films. They qualitatively demonstrate the thicknesses ratio of these films (the low transmittance of the SBN-50 film is due to the fact that free surface of the Al_2O_3 substrate was matted).

Comparison of the transmission curves in Fig. 2 indicates that all three SBN-61 films of different thicknesses have practically the same refractive indices. Processing of the transmission spectra for SBN-50 and the "thickest" SBN-61 films was performed in accordance with the following equations:

$$\sqrt{T_{\min}} = \frac{4nn_s}{(n^2 + n_s)(n_s + 1)}, \quad d = \frac{\lambda}{2} n(m + 1/2). \tag{6}$$

Here, $T_{\min}$ is the transmittance at the minimum points, n_s is the refractive index of the substrate material, taking into account its dispersion, and m is the order of interference (additional scattering on the free substrate surface was taken into account for SBN-50 film).

The refractive index value was estimated at maximum points after finding the average film thickness value. The order of interference and the refractive index $n_o \approx 2.3$ at the wavelength λ = 632.8 nm (m = 2 for SBN-50 and m = 3 for SBN-61), found from the transmission spectra, allowed us to determine the film thickness and its profile, and to refine the

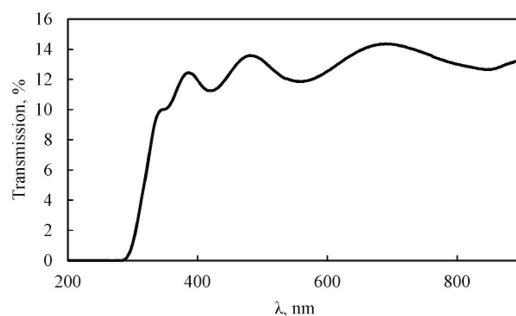

Fig. 1. Optical transmission spectrum of SBN-50/Al_2O_3 (Ref. 3) film.

J. Adv. Dielect. Downloaded from www.worldscientific.com by 95.24.11.130 on 10/16/21. Re-use and distribution is strictly not permitted, except for Open Access articles.

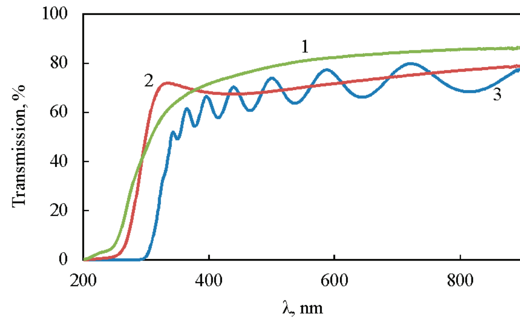

Fig. 2. Transmission spectra of SBN-61/MgO films: 1–5 min, 2–10 min and 3–115 min.

value of the refractive index at this wavelength by ellipsometry methods. In turn, the found film thickness allowed us to correct the estimated $n_o(\lambda)$. The field of experimental points that displays the dispersion for SBN-50 and SBN-61 films is shown in Fig. 3.

The Sellmeier equation was used to approximate this dependence in the weak absorption region:

$$n_{\circ}^2(\lambda)-1=\frac{S_0\lambda_0^2}{1-(\lambda_0/\lambda)^2}, \qquad (7)$$

where λ_0 is the average wavelength and S_0 is the average oscillator strength.

It can be seen from Fig. 3 that the observed dispersion in SBN-50 and SBN-61 films practically coincides with that for crystalline materials.[5] Refractive index values obtained from the transmission spectra at the wavelength of 632.8 nm were used as an initial approximation when processing the results of ellipsometric measurements. It has been found that the refractive index n_o is practically the same in all films. No boundary layers have been registered. The parameters of the damaged surface layers, namely the thickness d_{dis} and the effective refractive indices n_{ef}, as well as the corresponding volume-filling coefficient q, defined from Eq. (8), are determined,

$$\frac{n_{ef}^2-1}{n_{ef}^2+2}=q\frac{n^2-1}{n^2+2}. \qquad (8)$$

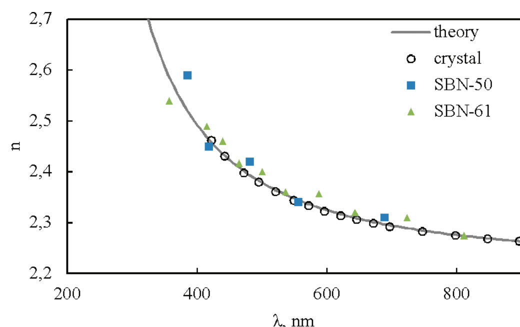

Fig. 3. Dispersion $n_o(\lambda)$ in SBN-50 and SBN-61 films.

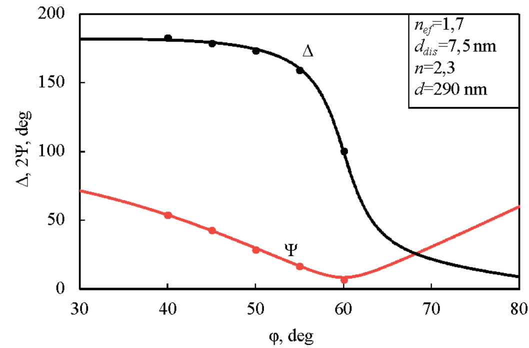

Fig. 4. $\psi(\varphi)$ and $\Delta(\varphi)$ dependences of the SBN-50/Al_2O_3 film: n_0 = 2.3 and d = 290 nm; damaged layer: n_{ef} = 1.7 and d_{dis} = 7.5 nm.

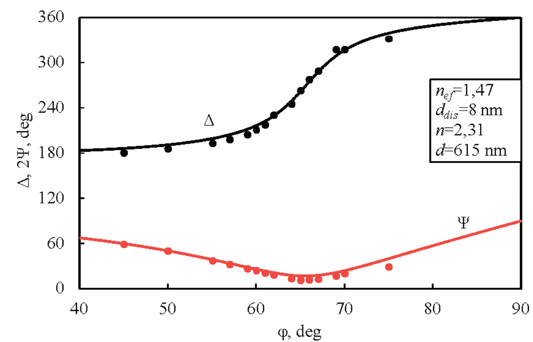

Fig. 5. $\psi(\varphi)$ and $\Delta(\varphi)$ dependences of the SBN-61/MgO film (t = 10 min): n_0 = 2.3 and d = 42 nm; damaged layer: n_{ef} = 1.65 and d_{dis} = 5 nm.

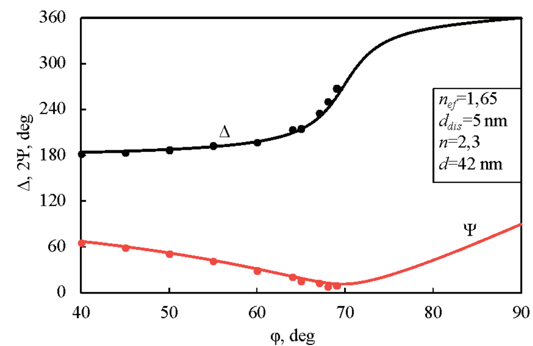

Fig. 6. $\psi(\varphi)$ and $\Delta(\varphi)$ dependences of the SBN-61/MgO film (t = 115 min): n_0 = 2.31 and d = 615 nm; damaged layer: n_{ef} = 1.47 and d_{dis} = 8 nm.

The ellipsometric angles ψ and Δ obtained from measurements of the polarizer and analyzer azimuths for SBN-50 (t = 30 min), SBN-61 (t = 10 min) and SBN-61 (t = 115 min) films are presented as examples in Figs. 4–6.

Calculated dependences $\psi(\varphi)$ and $\Delta(\varphi)$ from Eq. (1) with the input data shown in Table 1 are given here (Figs. 4–6). The SEM and AFM images of the film surface are shown in Fig. 7.

Table 1. Optical parameters of films.

Sample no.	d (nm)	$n = n_0$	Damaged layer n_{ef}	Damaged layer d_{dis} (nm)	Volume-filling coefficient (q)
—	290	2.3	1.7	7.5	0.625
1	29	2.3	1.65	5	0.6
2	42	2.3	1.65	5	0.6
3	615	2.31	1.47	8	0.45

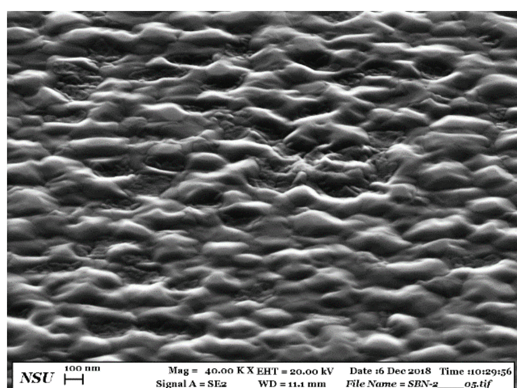

(a)

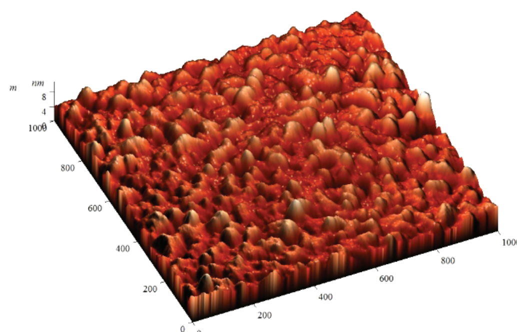

(b)

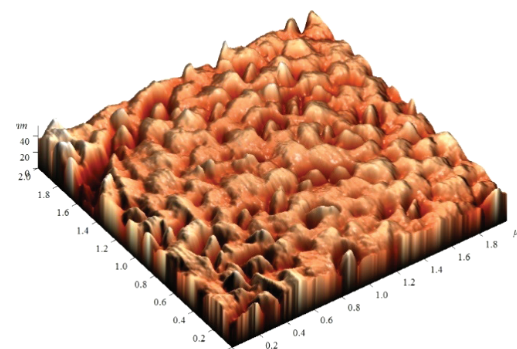

(c)

Fig. 7. (a) SEM image of SBN-50/Al_2O_3 film and (b), (c) surface morphologies of SBN-61 films (t = 10 min and 115 min, respectively).

These dependences demonstrate good agreement between the experimental results and the chosen theoretical approach. They confirm the correctness of the assumed model in relation to the barium–strontium niobate films. As can be seen from Table 1, the refractive indices and profiles of all films practically do not differ. At the same time, a slight increase in the thickness of the surface-damaged layer is observed. In addition, the refractive index of the "thickest" film approaches the n_0 value of the $Sr_{0.61}Ba_{0.39}Nb_2O_6$ crystal at a wavelength of 632.8 nm.[6,7] SEM studies of the films' surface morphology confirm the results of ellipsometry on the nature of the films' damaged layer depending on their thickness (Fig. 7). As shown by X-ray diffraction, the SBN-50/Al_2O_3 (0001) film is c-oriented, and the crystallographic axes of the film and the substrate are stochastically distributed in the interface plane (no signs of oriented growth have been detected during the φ-scan). This explains the "hilly" surface relief [Fig. 7(a)], which is formed during the intergrowth of film crystallites. The fact that we do not fix pronounced traces of the buffer layer at the film–substrate interface or the $SrNb_2O_6$ layer indicates that the deformations that occur in the film during the synthesis of heterostructure are quenched in the thick layer.[6] Most likely, an important role in this case is played by the fact that the film growth occurs at high oxygen pressures, which contributes, on the one hand, to the maximum elimination of nonstoichiometry and a decrease in defect structure due to oxygen vacancies, and, on the other hand, to the appearance of impurity phases.

In turn, SBN-61/MgO (001) films are heteroepitaxial and grown by the Vollmer–Weber mechanism.[5] That is, their relief, as can be seen from Figs. 7(b) and 7(c), increases with the growth of the film thickness, due to the specifics of the single-crystal film growth. An increase in the thickness of the damaged surface layer, established by optical studies, is accompanied by a simultaneous decrease in the volume-filling coefficient as the deposition time of SBN-61 films on MgO (001) increases. This suggests that the nature of the surface formation changes during the synthesis process, which is due to the peculiarity of the film growth. We plan to study this effect in more detail in future works.

5. Conclusions

1. It was established by ellipsometry methods that all investigated thin films SBN-61/MgO (001), regardless of thickness, as well as the SBN-50/Al_2O_3 (0001) film[3] are epitaxial with a predominant growth direction parallel to the c-axis of the single crystal. It was shown that anisotropy practically does not affect the results of ellipsometric measurements.
2. The film parameters of different thicknesses — refractive index, thickness of the base and surface-damaged layers and volume-filling coefficient of the damaged layer by the material — have been determined. The absence of a layer has been established at the film–substrate interface.

J. Adv. Dielect. Downloaded from www.worldscientific.com by 95.24.11.130 on 10/16/21. Re-use and distribution is strictly not permitted, except for Open Access articles.

3. It has been discovered that the thickness of the damaged layer grows and the volume-filling coefficient decreases with increasing film thickness. A natural tendency of an increase in the refractive index, approaching its maximum value in the bulk material for a given composition[7] as the film thickness increases, is observed.

It is advisable to use the results obtained in the development of optical elements based on barium–strontium niobates thin films.

Acknowledgments

The authors are grateful to V. B. Shirokov for conducting studies of the films surface by the AFM method. This work was carried out within the framework of the State Assignment of the SSC RAS (Theme of State Registration No. 01201354247).

References

[1]A. V. Rzhanov, K. K. Svitashev, A. I. Semenenko, L. V. Semenenko and V. K. Sokolov, *Osnovy Ellipsometrii* (Nauka, Novosibirsk, 1978).

[2]A. A. Tikhii, V. A. Gritckikh, S. V. Kara-Murza, N. V. Korchikova, Iu. M. Nikolaenko, V. V. Faraponov and I. V. Zhikharev, Ellipsometricheskii metod opredeleniia opticheskikh parametrov tonkoplenochnykh pokrytii so slozhnoi strukturoi, *Opt. Spektrosk.* **119**(2), 282 (2015).

[3]A. V. Pavlenko, S. V. Kara-Murza, A. P. Kovtun, N. V. Korchikova, A. A. Tikhii and D. V. Stryukov, Structure and optical characteristics of barium–strontium niobate films on Al_2O_3 substrates, *Opt. Spectrosc.* **126**, 487 (2019).

[4]A. P. Kovtun, S. P. Zinchenko, A. V. Pavlenko and G. N. Tolmachev, Opticheskaia anizotropiia i dielektricheskie kharakteristiki plenok $Sr_{0.50}Ba_{0.50}Nb_2O_6$/Pt(111)/Si(001), *Pis'ma Zh. Tekh. Fiz.* **42**(11), 48 (2016).

[5]Iu. S. Kuzminov, *Segnetoelektricheskie Kristally Dlia Upravleniia Lazernym Izlucheniem* (Nauka, Moskva, 1982).

[6]P. V. Lenzo, E. G. Spencer and A. A. Ballman, Electro-optic coefficients of ferroelectrics strontium barium niobate, *Appl. Phys. Lett.* **11**(1), 23 (1967).

[7]D. Kip, S. Aulkevye, K. Buse, F. Mersch, R. Panlrath and E. Kratziom, Refractive indices of $Ba_{0.61}Sr_{0.39}Nb_2O_6$ single crystals, *Phys. Status Solidi A* **151**, K3 (1996).

J. Adv. Dielect. Downloaded from www.worldscientific.com
by 95.24.11.130 on 10/16/21. Re-use and distribution is strictly not permitted, except for Open Access articles.